scientific reports

Check for updates

OPEN

Dual antibiotic PLGA microspheres for the treatment of traumatic osteomyelitis

Liangguo Si[1], Wenping Zhang[2], Haifeng Jiang[2], Haiqiang Ma[1], Xu Ma[1], Peijie Zhao[1], Huanhuan Sun[1], Zhipeng Yang[1] & Zewen Qiao[2]✉

Traumatic osteomyelitis (TO) treatment remains challenging due to biofilm formation and poor antibiotic penetration. We developed poly(lactic-co-glycolic acid) (PLGA) microspheres co-loaded with moxifloxacin/rifampicin (M/R-P) to address these limitations. Key findings: In vitro: The microspheres showed (1) no cytotoxicity (CCK-8 assay; live/dead staining; cytoskeletal staining; SEM visualization), and (2) no inhibition of osteogenic potential (ALP activity).In vivo: M/R-P microspheres significantly reduced MRSA burden ($8 \pm 3 \times 10^3$ CFU/g) compared to debridement-only controls ($3143 \pm 727 \times 10^3$ CFU/g; $p < 0.0001$), and near-complete infection resolution (histopathology). Conclusion: These results demonstrate that the M/R-P microspheres possess excellent safety profiles, favorable cytocompatibility, and remarkable antibacterial efficacy. The findings confirm the feasibility of our innovative approach using PLGA as a drug delivery carrier for localized antibiotic therapy in chronic osteomyelitis treatment, achieved through technological optimization for combined antibiotic administration. This provides a novel strategic direction for ultimately overcoming the clinical challenge of traumatic osteomyelitis.

Keywords PLGA, Moxifloxacin, Rifampicin, Osteomyelitis, Localized drug delivery, MRSA

Traumatic osteomyelitis (TO) represents one of the most clinically challenging bone infections, with common etiologies including open fractures, hematogenous bacterial dissemination, and perioperative contamination during orthopedic procedures[1].Infection constitutes the primary cause of nonunion in open fractures and the leading reason for failure in joint replacement surgeries[2]. Notably, approximately 40% of patients with bone infections develop recurrent or chronic infections[3].Patients with TO typically require multiple surgical interventions, endure prolonged treatment courses, and face high recurrence rates with poor prognoses—all contributing to significant psychological distress and socioeconomic burdens[4].

The treatment of traumatic osteomyelitis presents significant clinical challenges. While traditional approaches including repeated debridement and systemic antibiotic administration can provide partial infection control, they frequently fail to substantially shorten treatment duration or reduce recurrence rates[5]. Two pathophysiological barriers primarily account for these therapeutic difficulties: First, the compromised local microenvironment perpetuates infection. Trauma-induced tissue damage creates an ideal niche for bacterial colonization and dissemination[6]. The resulting ischemic conditions severely limit antibiotic penetration to therapeutic concentrations[7], making protection of compromised tissues critically important[8]. This microenvironment not only fosters bacterial resistance but also complicates dose escalation due to systemic toxicity.Second, the virulence mechanisms of predominant pathogens prove particularly formidable. Staphylococcus aureus (S. aureus), responsible for approximately 75% of TO cases[9], employs sophisticated evasion strategies including biofilm formation and host cell internalization[10]. Biofilms establish protective microenvironments within hours of infection, enhancing bacterial survival while promoting proliferation[11,12]. Through invasion of osteoblasts, fibroblasts, and endothelial cells, S. aureus evades immune clearance while inducing host cell necrosis—thereby generating new bacterial adhesion sites[13]. These mechanisms underscore why current research prioritizes enhancing local antibiotic delivery alongside surgical debridement[14].

Local antibiotic delivery has emerged as a cornerstone therapeutic strategy, achieving high lesion-site concentrations while minimizing systemic exposure[15]. Since Buchholz and Engelbrecht's seminal 1970 demonstration of antibiotic-loaded bone cement efficacy (reducing infection rates from 6–1.6%)[16], this approach has gained widespread adoption. However, limitations including poor antibiotic elution, narrow spectrum coverage, and non-degradability[17–19] may contribute to treatment failure and resistance development[20].

[1]School of Clinical Medicine, Ningxia Medical University , 750004 Yinchuan, China. [2]General Hospital of Ningxia Medical University, 750004 Yinchuan, China. ✉email: 13995307859@163.com

These shortcomings have driven innovation in biodegradable, sustained-release platforms[21–24], among which poly(lactic-co-glycolic acid) (PLGA) excels due to its excellent biocompatibility, predictable degradation kinetics, and minimal immunogenicity[25].

The bacteriological profile of TO demonstrates S. aureus predominance alongside environment-dependent pathogens[26]. In this era of escalating resistance, optimal antibiotic selection must balance broad-spectrum coverage with target specificity[27]. Moxifloxacin (MOX), a fourth-generation fluoroquinolone, exerts bactericidal effects through specific inhibition of bacterial DNA gyrase and topoisomerase IV. This mechanism effectively suppresses biofilm formation by Staphylococcus aureus and Pseudomonas aeruginosa while enabling penetration through established biofilm matrices[28].Conversely, rifampicin (RIF)acts by binding the β-subunit of bacterial RNA polymerase, disrupting transcription. This agent demonstrates exceptional tissue penetration and intracellular bactericidal activity, including potent efficacy against biofilm-embedded microorganisms[29,30].The combined application of MOX and RIF can significantly improve the antibacterial effect[31].While numerous advanced drug delivery platforms have been developed for antibiotic encapsulation[32–34], the majority of existing research has focused on single-antibiotic systems, with few reports addressing co-delivery of multiple antimicrobial agents. In our previous research, through technological innovation, we simultaneously encapsulated MOX and RIF in PLGA to prepare M/R-P microspheres. We evaluated and reported the characterization, drug sustained release, and in vitro antibacterial rate of the microspheres. Both quantitative and qualitative antibacterial assessments demonstrated that the dual drug-loaded microspheres exhibited superior antibacterial activity compared to single drug-loaded formulations[35]. This study aims to achieve the combined application of antibiotics by optimizing the PLGA vector technology, improve the therapeutic effect of local treatment for chronic bone infections, and provide a new idea for completely solving the problem of traumatic bone infections in the future.

Materials & methods

Materials

PLGA (50:50 lactide: glycolide, MW 10 kDa; Shandong Medical Instrument Co.). RIF and MOX were purchased from Sigma-Aldrich (USA). The Cell Counting Kit-8 (CCK-8) and alkaline phosphatase (ALP) assay kit were acquired from Beijing Solaibao Technology Co., Ltd. (China). All other reagents were obtained from Sigma-Aldrich and used without further purification.

Preparation of microspheres

M-P (MOX-loaded) and M/R-P microspheres were prepared using our previously reported method[35]. Briefly, 240 mg PLGA and 30 mg RIF were dissolved in dichloromethane (DCM) as the oil phase (O). One milliliter of MOX solution (30 mg/mL) served as the internal water phase (W1), which was emulsified into the oil phase under continuous stirring to form a primary water-in-oil emulsion (W1/O). This emulsion was then added to 40 mL of 1% polyvinyl alcohol (PVA) solution and homogenized to form a double emulsion (W1/O/W2). The resulting emulsion was transferred into 800 mL of 0.5% PVA solution and stirred for 10 h to allow solvent evaporation.The microspheres were collected by centrifugation (12,000 rpm, 10 min), washed three times with deionized water, and lyophilized (Scientz-10 N, Ningbo Xinzhi Biotechnology Co., Ltd.) at −40 °C for 24 h. M-P microspheres were prepared similarly without rifampicin. All microspheres were stored in light-protected containers at 4 °C until use.The drug loading capacity of MOX-PLGA microspheres was 2.10% ± 0.12%, with an encapsulation efficiency of 17.35% ± 2.42%. For M/R-P microspheres, the loading capacities were 3.42% ± 0.74% (MOX) and 5.03% ± 0.85% (RIF), with encapsulation efficiencies of 33.25% ± 7.51% and 49.0% ± 11.25%, respectively. Prior to use, all microspheres were sterilized by γ-irradiation (25 kGy total dose, delivered at 5 kGy/h for 5 h) under nitrogen-purged vacuum packaging.

.

Cell culture

Human bone marrow-derived mesenchymal stem cells (hMSCs; Cyagen Biosciences, Shanghai, China) were cultured in α-minimum essential medium (α-MEM) supplemented with 10% fetal bovine serum (FBS), 100 U/mL penicillin, and 100 μg/mL streptomycin at 37 °C in a humidified 5% CO_2 atmosphere. The medium was refreshed every 48 h, and passage 3 cells were used for all experiments.

In vitro cytocompatibility evaluation

Cell viability assay (CCK-8)

hMSCs (1×10^4 cells/well) were seeded in 96-well plates with 5 mg microspheres/well ($n = 6$ per group). Control wells contained cells only. After 3 and 7 days, cells were washed with PBS and incubated with 100 μL α-MEM containing 10 μL CCK-8 reagent for 30 min. Absorbance was measured at 450 nm using a microplate reader.

Alkaline phosphatase (ALP) activity

Following the same seeding protocol, after the cells adhered to the wall for 24 h, cells were cultured in osteogenic induction medium (Guangzhou Saiye Biotechnology Co., Ltd.) for 3 and 7 days. Cells were lysed with 0.1% Triton X-100, and ALP activity in the supernatant was measured using p-nitrophenyl phosphate as substrate (absorbance at 520 nm).

Scanning electron microscopy (SEM)

hMSCs (1×10^4 cells/mL) were co-cultured with microspheres on cell culture slides for 3 and 7 days. Samples were fixed with 2.5% glutaraldehyde (12 h), dehydrated in an ethanol series, critical-point dried, sputter-coated with gold, and imaged using SEM (Hitachi SU8010, Japan).

Live/dead staining
Cells were stained with Calcein-AM (2 μM) and propidium iodide (4.5 μM) for 20 min at room temperature. Fluorescence images were acquired using confocal laser scanning microscopy (CLSM; Zeiss LSM 880, Germany).

Cytoskeletal staining
Cells were fixed with 4% paraformaldehyde, permeabilized with 0.4% Triton X-100, stained with FITC-phalloidin (1:200) and DAPI (1 μg/mL), and imaged by CLSM.

In vivo therapeutic efficacy assessment

Bacterial culture
Methicillin-resistant Staphylococcus aureus (MRSA; Purity Biotechnology, Wuhan, China) was cultured on LB agar at 37 °C for 24 h. Bacterial suspensions (1.2×10^7 CFU/mL in PBS) were prepared for animal inoculation.

Initiate of animal model of TO
All animal experiments were approved by the Institutional Animal Protection and Use Committee of Ningxia Medical University (No. 2020-0001). Twenty-four male SD rats (4 weeks old, weighing 160–180 g, purchased from the Animal Experiment Center of Ningxia Medical University) were used to establish the animal model of osteomyelitis[36].Rats stratified by weight using block randomization (GraphPad), Radiographic scoring performed by two independent blinded veterinarians, Buprenorphine (0.05 mg/kg) administered pre-op and q12h × 48 h, One control-group rat died at week 6 (infection) and was excluded.

The animals were anesthetized with isoflurane (RWD, China), and the proximal tibial metaphysis was exposed through an anteromedial incision of the right knee. A bone marrow cavity was created using a bone drill, into which a Kirschner wire (approximately 5.0 × 1.0 mm) was implanted. Subsequently, 0.2 mL of MRSA suspension (1.2×10^7 CFU/mL) was injected into the cavity. The defect was sealed with bone wax, irrigated three times with normal saline, and the wound was sutured. No antibiotics were administered during or after the procedure.

Postoperatively, three rats were randomly selected for radiographic confirmation of Kirschner wire placement. Then all the rats were randomly divided into 3 groups($n = 8$ per group). At week 4, three rats from each group underwent imaging examination followed by euthanasia for pathological specimen collection. The remaining animals received surgical intervention consisting of Kirschner wire removal and thorough debridement to excise all necrotic tissue. The treatment groups received either M/R-P or M-P microsphere implantation, while the control group received debridement only. At week 8, three rats per group were sacrificed after imaging for final pathological evaluation.Clarify that 8-week data = 4 weeks post-treatment.

At experimental endpoints, rats were humanely euthanized via intraperitoneal injection of pentobarbital sodium (150 mg/kg) following AVMA guidelines. Death was confirmed by absence of corneal reflex and cessation of heartbeat.

Radiographic analysis
X-ray and CT scans were performed at 0, 4, and 8 weeks. osteomyelitic changes were scored using Norden's criteria[37].

Bacterial load quantification
Infected bone tissues were homogenized, serially diluted, plated on LB agar, and incubated at 37 °C for 24 h. Colony-forming units (CFU) per gram of bone were calculated.

Histopathological examination
Tissues were fixed in 4% paraformaldehyde, decalcified in 10% EDTA (pH 7.4) for 6 weeks, paraffin-embedded, sectioned (5 μm), and stained with: H&E: Inflammatory cell infiltration and bone destruction; Masson's trichrome: Collagen deposition and bone remodeling.Images were acquired using a Nikon Eclipse Ti microscope (Japan).

Statistical analysis

Data were analyzed by two-way ANOVA using GraphPad Prism 9.0 and presented as mean ± SD ($n \geq 3$). Significance was set at $^*p < 0.05$, $^{**}p < 0.01$, $^{***}p < 0.001$, and $^{****}p < 0.0001$; "ns" denotes not significant. Intergroup differences at the same time point are indicated by *, while temporal differences within groups are marked by #.

Result

In vitro cytocompatibility of microspheres

The CCK-8 assay demonstrated progressive cell proliferation across all groups over time ($P < 0.0001$). No significant differences in cell viability were observed among groups at either 3-day or 7-day time points ($P > 0.05$, Fig. 1A), indicating that microsphere addition of microspheres did not affect hMSC proliferation.

Alkaline phosphatase (ALP) activity, a key marker of early osteogenic differentiation, showed temporal increases in all groups under osteoinductive conditions ($P < 0.0001$). Similar to proliferation results, no intergroup differences in ALP activity were detected at either time point ($P > 0.05$, Fig. 1B), confirming that microspheres did not impair osteogenic potential.

The SEM image (Fig. 2) observed that hMSCs could attach to microspheres for proliferation. 3D images of live and dead cells after staining (green fluorescence indicates live cells and red fluorescence indicates dead cells), as shown in Fig. 3, rarely can the red fluorescence symbolizing dead cells be observed.

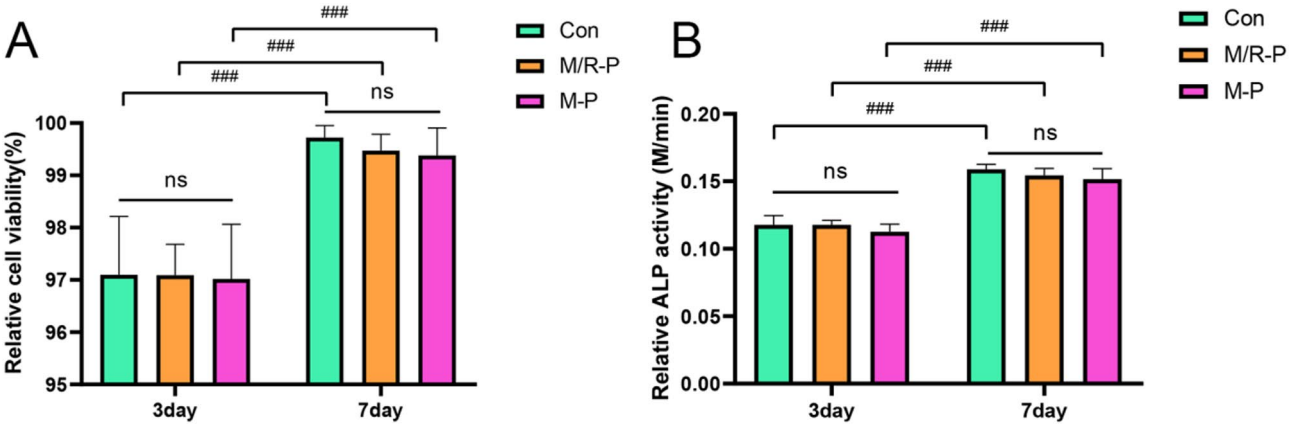

Fig. 1. After 3 and 7 days of co-culture of cells and microspheres, cell activity was detected by CCK-8 kit (Fig. 1A) and cell ALP value was detected by ALP kit (Fig. 1b).

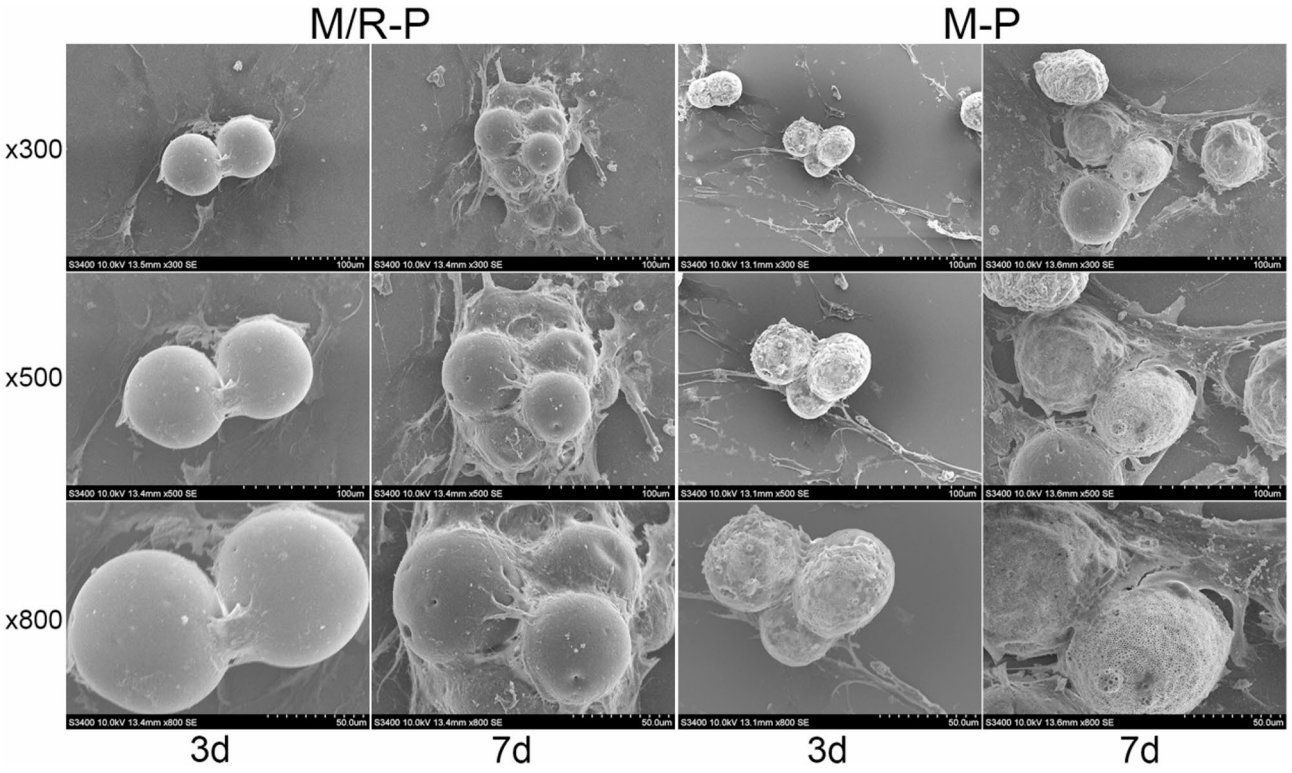

Fig. 2. SEM photos of M/R-P microspheres and M-P microspheres and cells co-cultured for 3 and 7 days, respectively.

The three groups of samples at two time periods were subjected to Cytoskeletal staining using TRITC-Phalloidin AF555 staining solution, and the cell nuclei were labeled with DAPI staining solution. The morphology of the cytoskeleton was observed. The 3D image (Fig. 4) shows that the hMSCs skeleton around the microspheres is intact.

In vivo therapeutic efficacy

Imaging evaluation

Serial radiographic assessments at 0, 4, and 8 weeks (Fig. 5) demonstrated: Week 0: Successful Kirschner wire placement in tibial marrow cavity. Week 4: Characteristic osteomyelitic changes in all groups, including: reduced bone density, peri-implant abscess formation, trabecular thinning/erosion, necrotic bone formation, periosteal reaction.Week 8:Control group: Progressive bone destruction with irregular reactive bone formation. M-P group: Mild remission. M/R-P group: The osteomyelitic symptoms demonstrated marked improvement, with

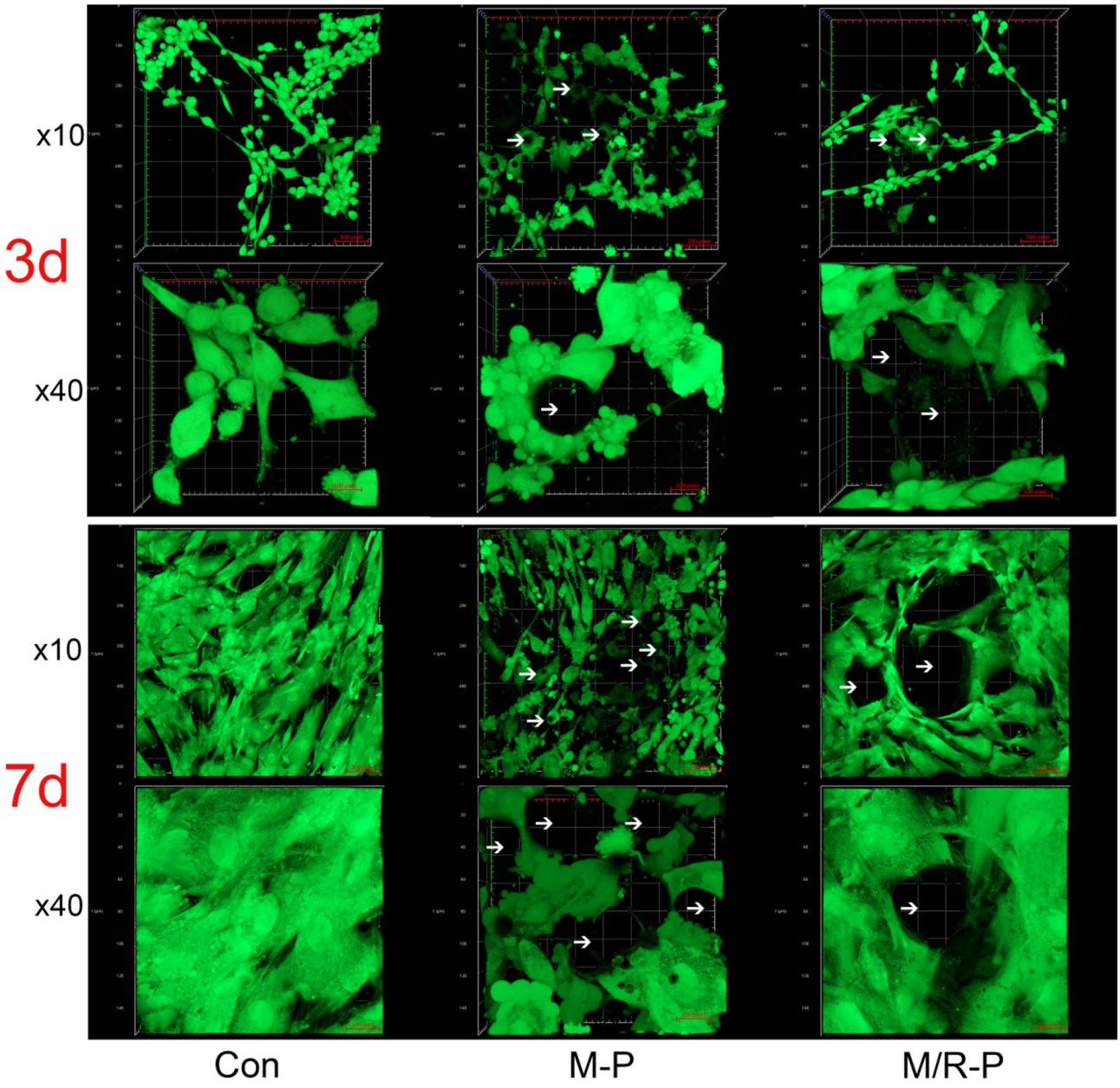

Fig. 3. 3D images of living and dead cells stained under CLSM after co-culture of M/R-P microspheres and M-P microspheres with cells for 3 and 7 days, respectively. The white arrows indicate the positions of the microspheres.

near-complete resolution of both osseous abscesses and lytic bone lesions.One control animal succumbed to severe infection during the study (Table 1).Clarify that 8-week data = 4 weeks post-treatment.

Using Norden's radiographic scoring system[37](Fig. 6A; Table 2):Week 4: All groups scored ≥ 4.5 ($P \geq 0.05$), confirming model establishment.Week 8:M/R-P: Scores ≤ 0.5 ($P < 0.0001$ vs. week 4), indicating near-complete resolution.M-P: Scores ≤ 3 ($P < 0.0001$ vs. week 4), showing partial improvement.Control: Scores ≥ 6 ($P = 0.0095$ vs. week 4), demonstrating progression.Intergroup comparisons at week 8 showed significant differences ($P < 0.0001$).

Bacterial quantification

Bacterial loads (CFU/g bone tissue)(Fig. 6B): Week 4:M/R-P: $833 \pm 96 \times 10^3$.M-P: $873 \pm 45 \times 10^3$.Control: $789 \pm 29 \times 10^3$.($P > 0.05$ among groups).Week 8:M/R-P: $8 \pm 3 \times 10^3$ ($P = 0.0085$ vs. week 4).M-P: $353 \pm 72 \times 10^3$ ($P = 0.1268$ vs. week 4).Control: $3143 \pm 727 \times 10^3$ ($P < 0.0001$ vs. week 4).Significant differences at week 8:M/R-P vs. control: $P < 0.0001$.M-P vs. control: $P < 0.0001$.Notably, M/R-P vs. M-P: $P = 0.2545$.

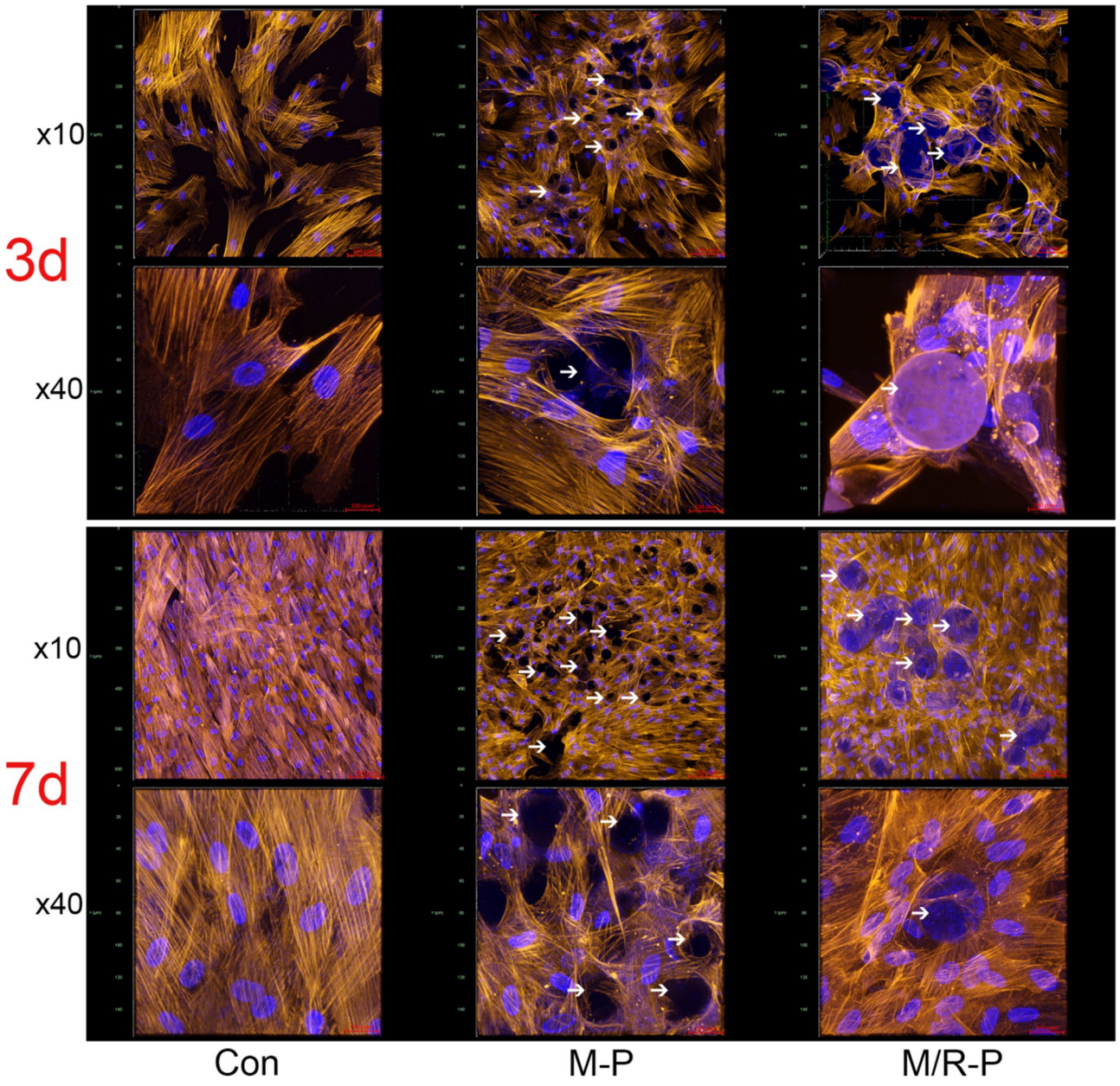

Fig. 4. 3D images of cytoskeletal protein staining after co-culture of M/R-P microspheres and M-P microspheres with cells for 3 and 7 days, respectively. The white arrows indicate the positions of the microspheres.

Histopathological assessment

H&E staining (Fig. 7):Week 4: all groups showed: extensive inflammatory infiltration, interstitial hemorrhage. abscess formation.Week 8:M/R-P: Reduced inflammation dramatically, Visible osteoblast rimming, Partial marrow reconstitution.M-P: Reduced inflammation mildly, Organized lymphoplasmacytic infiltrates.Control: Severe neutrophilic infiltration, Confluent abscess formation, Prominent osteolysis with empty lacunae, Marrow space obliteration by inflammatory exudate.

Masson's trichrome staining (Fig. 8):Week 4: All groups exhibited: Disrupted collagen architecture (blue stain), Minimal osteoid formation, Fragmented trabeculae.Week 8:M/R-P: Robust trabecular bone formation, Active osteoid seams, Bridging trabeculae formation.M-P: Organized collagen deposition.Control: Few collagen deposition, Advanced bone loss.

Discussion

Antibiotics play a pivotal role in osteomyelitis management; however, systemic intravenous administration often yields suboptimal therapeutic outcomes in TO due to multiple barriers including bacterial biofilm formation and ischemic conditions in infected regions[10,38]. Localized sustained-release antibiotic delivery systems have

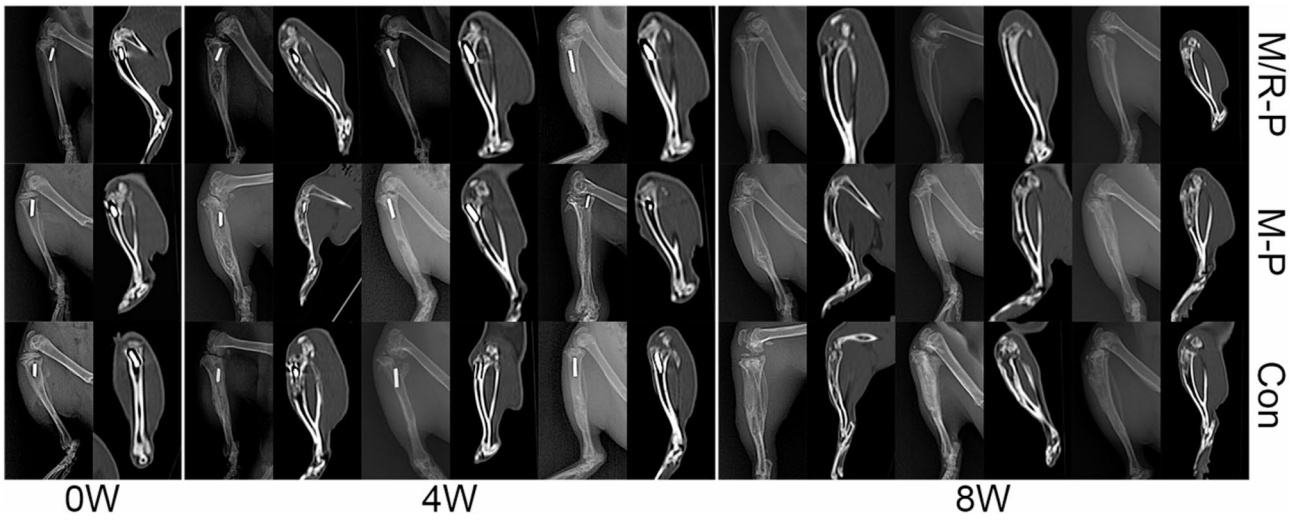

Fig. 5. X-ray and CT images of each group at week 0, week 4 and week 8.

Time	Rats		
	M/R-P	*M-P*	Con
0 W	8	8	8
4 W	5	5	5
8 W	5	5	4

Table 1. Schedule.

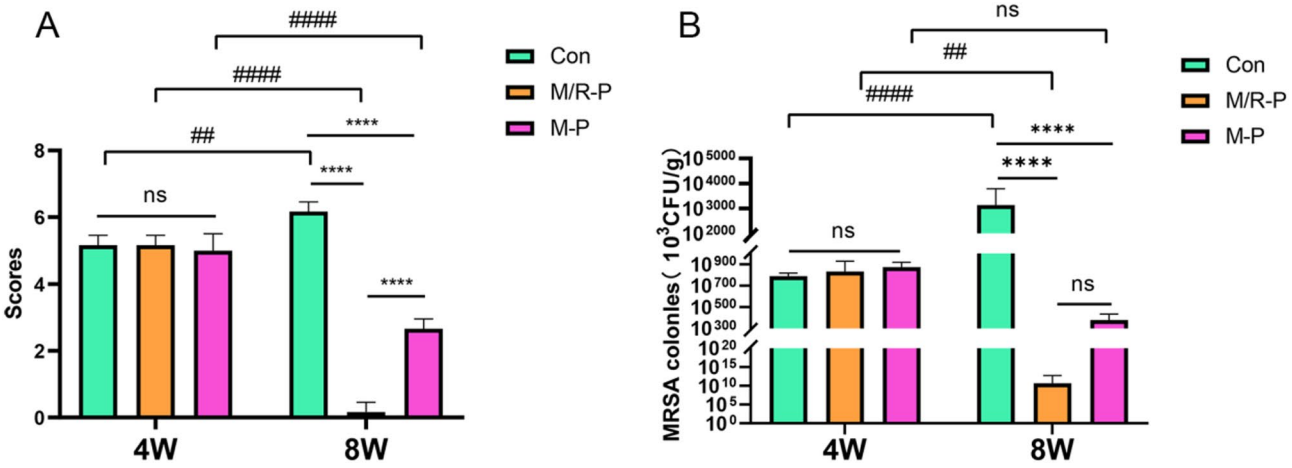

Fig. 6. (**A**) Imaging scores. (**B**) Statistical analysis of colony culture counts in the control group and the two microsphere groups.

emerged as a promising strategy to overcome these challenges, offering enhanced therapeutic efficacy while minimizing systemic toxicity[39]. While antibiotic-loaded poly(methyl methacrylate) (PMMA) remains the current clinical gold standard for osteomyelitis treatment, it presents several inherent limitations: (1) the release of antibiotics is limited and uneven, (2) incompatibility with a variety of antibiotics, (3) necessity for secondary removal surgery and potential reinfection risk. These drawbacks have driven the development of biodegradable alternatives capable of localized antibiotic delivery while promoting osteogenesis[40]. In our previous study, we successfully co-encapsulated RIF and MOX in PLGA microspheres (M/R-P), demonstrating favorable drug loading efficiency, sustained release kinetics, and potent antibacterial activity in vitro[35].The current study further validates the cytocompatibility and in vivo therapeutic efficacy of these microspheres.

	Variable	Definition	Point Score
I	Sequestrum formation	+ present - absent	1 0
II	Periosteal new bone formation	+ present ± equivocal - absent	1 0.5 0
III	Destruction of bone	++ severe, multiple areas involved + moderate, only one area involve(d ± mild, only one area inx-olved - no destruction	2 1 0.5 0
IV	Extent of disease: involvement of each of three areas (proximal, mid, and distal tibia)	+ present ± equivocal - absent	1 0.5 0

Table 2. Oentgenographic criteria.

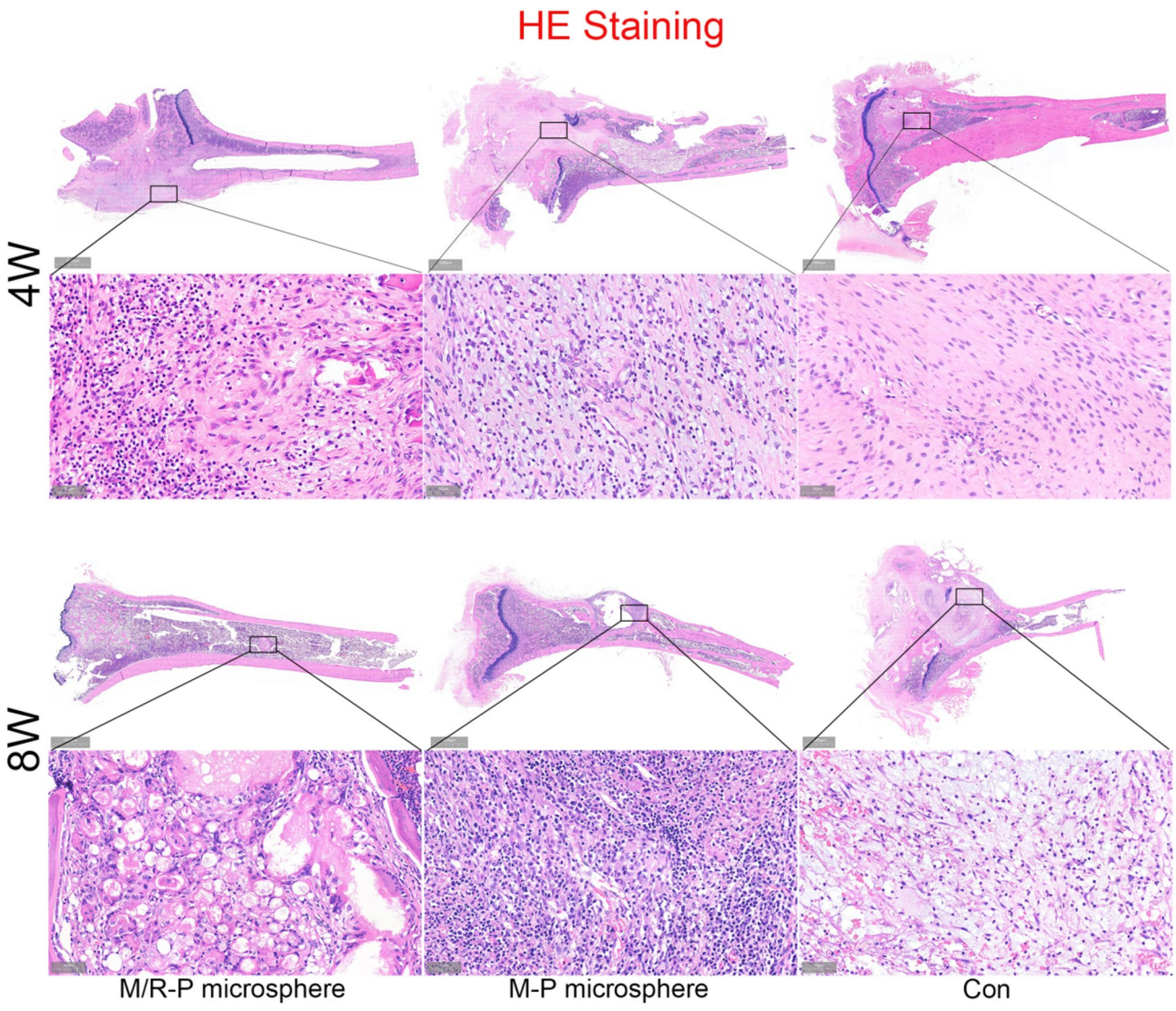

Fig. 7. Pathological images of HE staining of rats in each group.

PLGA has gained prominence in biomedical applications due to its excellent biocompatibility and tunable degradation properties. As its degradation products (lactic and glycolic acids) are endogenous metabolites, PLGA offers superior biosafety profiles[41,42]. However, excessive accumulation of acidic degradation byproducts may locally decrease tissue pH, potentially triggering inflammatory responses and impairing osteogenesis—thereby hindering bone infection resolution[9,43]. Our in vitro cytocompatibility assessments with hMSCs revealed no significant adverse effects of PLGA microspheres or their degradation products on cell proliferation, adhesion,

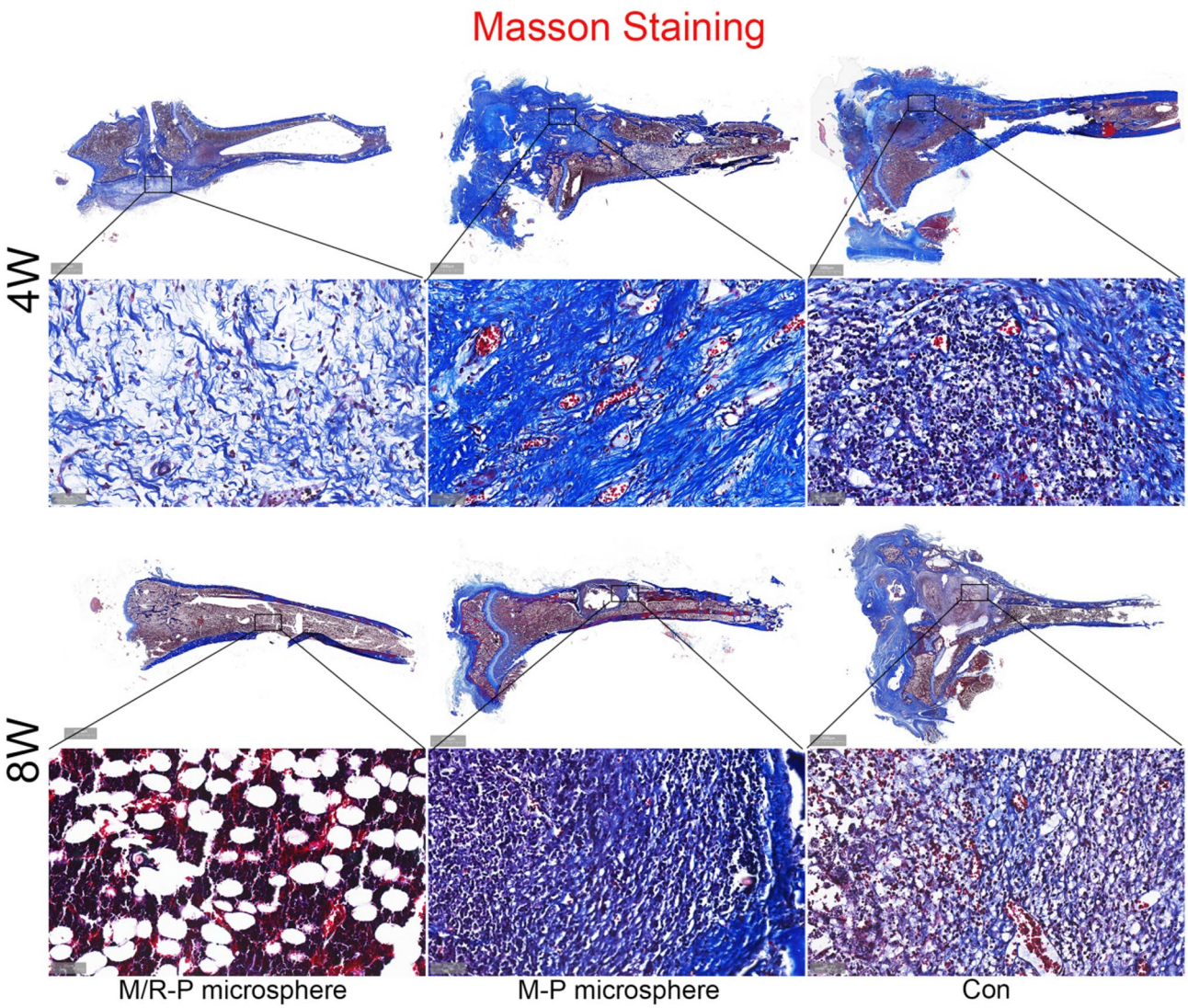

Fig. 8. Masson staining pathological images of rats in each group.

or osteogenic differentiation (as measured by ALP activity). These findings align with most published reports, though it should be noted that existing literature suggests potential cell viability inhibition due to excessive acidification from rapid PLGA degradation[44]. To avoid this problem, we chose high-molecular-weight PLGA for the preparation of microspheres, as the degradation rate of PLGA is related to its own molecular weight. The higher the molecular weight, the slower the degradation[45].

Severe open fractures and implant-related procedures represent major risk factors for traumatic bone infections[46], with S. aureus being the predominant pathogen[2,13,45]. In this study, we successfully established a clinically significant TO model by surgically implanting Kirschler needles and introducing MRSA into the tibia of rats[47]. In clinical practice, the acute phase of TO (prior to sequestrum formation) typically responds well to surgical debridement combined with systemic intravenous antibiotics[39], making this stage less therapeutically challenging. Consistent with previous studies, our intervention targeted the chronic phase of bone infection characterized by radiographic evidence of bone destruction, sequestrum formation, and sclerotic changes—conditions where systemic antibiotic penetration becomes severely limited[36,48]. The in vivo results demonstrated superior infection control in the M/R-P microsphere group compared to controls. The limited therapeutic efficacy observed in the M-P group may be attributed to the relatively low encapsulation efficiency of MOX, resulting in suboptimal local drug concentrations. Notably, during microsphere preparation, we found that co-encapsulation of hydrophobic RIF with hydrophilic MOX significantly enhanced drug loading capacity compared to MOX encapsulation alone. However, whether such hydrophilic-hydrophobic drug co-encapsulation universally improves encapsulation efficiency remains unexplored in current literature, with no existing reports addressing this specific phenomenon.

The M/R-P treatment group exhibited the most pronounced symptomatic improvement, likely attributable to comprehensive bacterial clearance that established a pro-regenerative microenvironment for endogenous bone repair. While RIF has been reported to promote M2 macrophage polarization—potentially contributing to

both anti-inflammatory effects and osteogenesis[49]—the exact immunomodulatory mechanisms in TO warrant further investigation to fully harness its therapeutic potential in bone repair[50].

Although positive experimental results were achieved, this experiment has many limitations: In the staining experiment of live and dead cells, we only set up the M/R-P group, the M-P group, and the control group with only cells, and did not set up a negative control group. In order to observe the growth state of cells and microspheres after co-culture, all our fluorescence images were 3D images. Due to technical limitations, fluorescence quantitative analysis could not be carried out.In vivo PLGA degradation and local pH changes were not quantified; future studies should measure inflammatory cytokines (e.g., IL-6, TNF-α).Furthermore, in animal experiments, the number of animals we used was relatively small, quantitative radiographic analysis was not systematically performed, while bone regeneration was inferred from histology but requires μCT confirmation. Moreover, traumatic bone infections are usually combined with osteonecrosis and bone defects. Although the use of M/R-P microspheres alone can effectively control the infection, it does not promote osteogenesis. In our future research, adding bone-promoting components such as magnesium ions to microspheres, or combining them with scaffolds such as hydroxyapatite/chitosan, collagen/BMP-2, etc., to have both anti-infection and bone regeneration capabilities will be our research focus.

Conclusion

Based on the previous studies, this research further conducted studies on the cytocompatibility and in vivo therapeutic effects of microspheres, and completed a series of studies on the preparation, properties, in vitro antibacterial and cytocompatibility, and in vivo treatment of traumatic bone infections in animals of M/R-P microspheres. Although the experimental results have many limitations, this study proved the feasibility of the concept of using PLGA as a carrier encapsulate two antibiotics and achieve the combined application of antibiotics in local treatment of TO. It provides a new idea for thoroughly solving the problem of TO in the future.

Data availability

All data generated or analysed during this study are includedin this published article and its supplementary information files.

Received: 21 March 2025; Accepted: 4 August 2025
Published online: 21 August 2025

References

1. Decoster, T. A. & Bozorgnia, S. Antibiotic beads. *J. Am. Acad. Orthop. Surg.* **16** (11), 674–678 (2008).
2. Urish, K. L. & Cassat, J. E. *staphylococcus aureus osteomyelitis: bone, bugs, and surgery*. *Infect. Immun.* **88**(7), (2020).
3. Feng, X. et al. Ultrasonic interfacial engineering of MoS(2) -Modified Zn Single-Atom catalysts for efficient osteomyelitis sonodynamic ion therapy. *Small* **18** (8), e2105775 (2022).
4. O'Connor, O., Thahir, A. & Krkovic, M. How much does an infected fracture cost?? *Arch. Bone Jt. Surg.* **10** (2), 135–140 (2022).
5. Kankilic, B. et al. Vancomycin containing PLLA/β-TCP controls experimental osteomyelitis in vivo. *J. Orthop. Surg. Res.* **9**, 114 (2014).
6. De Meo, D. et al. Candida fracture-related infection: a systematic review. *J. Bone Jt. Infect.* **6** (7), 321–328 (2021).
7. Wahlig, H. et al. The release of gentamicin from polymethylmethacrylate beads. An experimental and Pharmacokinetic study. *J. Bone Joint Surg. Br.* **60-b** (2), 270–275 (1978).
8. Guarnieri, R. et al. In vitro direct and indirect cytotoxicity comparative analysis of one pre-hydrated versus one dried acellular porcine dermal matrix. *Mater. (Basel)* **15**(5), (2022).
9. Tang, R. H., Yang, J. & Fei, J. New perspectives on traumatic bone infections. *Chin. J. Traumatol.* **23** (6), 314–318 (2020).
10. Gogia, J. S. et al. Local antibiotic therapy in osteomyelitis. *Semin Plast. Surg.* **23** (2), 100–107 (2009).
11. Metsemakers, W. J. et al. Infection after fracture fixation: current surgical and Microbiological concepts. *Injury* **49** (3), 511–522 (2018).
12. Barberán, J. et al. Conservative treatment of Staphylococcal prosthetic joint infections in elderly patients. *Am. J. Med.* **119** (11), 993e7–99310 (2006).
13. Masters, E. A. et al. Skeletal infections: microbial pathogenesis, immunity and clinical management. *Nat. Rev. Microbiol.* **20** (7), 385–400 (2022).
14. Posadowska, U., Brzychczy-Włoch, M. & Pamuła, E. Gentamicin loaded PLGA nanoparticles as local drug delivery system for the osteomyelitis treatment. *Acta Bioeng. Biomech.* **17** (3), 41–48 (2015).
15. Schentag, J. J. et al. Comparative tissue accumulation of gentamicin and tobramycin in patients. *J. Antimicrob. Chemother.* **4** (Suppl A), 23–30 (1978).
16. Buchholz, H. W., Elson, R. A. & Heinert, K. Antibiotic-loaded acrylic cement: current concepts. *Clin. Orthop. Relat. Res.* **190**, 96–108 (1984).
17. Martínez-Moreno, J. et al. Antibiotic-loaded bone cement as prophylaxis in total joint replacement. *Orthop. Surg.* **9** (4), 331–341 (2017).
18. Lee, S. H. et al. Elution and mechanical strength of Vancomycin-Loaded bone cement: in vitro study of the influence of brand combination. *PLoS One.* **11** (11), e0166545 (2016).
19. Parra-Ruíz, F. J. et al. Development of advanced biantibiotic loaded bone cement spacers for arthroplasty associated infections. *Int. J. Pharm.* **522** (1–2), 11–20 (2017).
20. Metsemakers, W. et al. New definition for periprosthetic joint infection: from the workgroup of the musculoskeletal infection society. (2016).
21. Ferguson, J. Y. et al. The use of a biodegradable antibiotic-loaded calcium sulphate carrier containing tobramycin for the treatment of chronic osteomyelitis: a series of 195 cases. *Bone Joint J.* **96-b** (6), 829–836 (2014).
22. Inzana, J. A. et al. Biomaterials approaches to treating implant-associated osteomyelitis. *Biomaterials* **81**, 58–71 (2016).
23. Beuerlein, M. J. & McKee, M. D. Calcium sulfates: what is the evidence? *J. Orthop. Trauma.* **24** (Suppl 1), S46–51 (2010).
24. McKee, M. D. et al. The use of an antibiotic-impregnated, osteoconductive, bioabsorbable bone substitute in the treatment of infected long bone defects: early results of a prospective trial. *J. Orthop. Trauma.* **16** (9), 622–627 (2002).
25. Singh, Y. et al. Nanoemulsion: concepts, development and applications in drug delivery. *J. Control Release.* **252**, 28–49 (2017).
26. Dudareva, M. et al. The microbiology of chronic osteomyelitis: changes over ten years. *J. Infect.* **79** (3), 189–198 (2019).

27. Ozturk, I. et al. In vitro effect of Moxifloxacin and rifampicin on biofilm formation by clinical MRSA isolates. *Bratisl Lek Listy*. **115** (8), 483–486 (2014).
28. Zelmer, A. R. et al. Can intracellular Staphylococcus aureus in osteomyelitis be treated using current antibiotics? A systematic review and narrative synthesis. *Bone Res.* **10** (1), 53 (2022).
29. Chambers, H. F. Rifabutin to the rescue?? *J. Infect. Dis.* **222** (9), 1422–1424 (2020).
30. Zelmer, A. R. et al. Osteomyelitis-relevant antibiotics at clinical concentrations show limited effectivity against acute and chronic intracellular S. aureus infections in osteocytes. *Antimicrob. Agents Chemother.* **68** (10), e0080824 (2024).
31. Kurbatova, E. V. et al. Efficacy and safety of 4-Month Rifapentine-Based tuberculosis treatments in persons with diabetes. *Emerg. Infect. Dis.* **31** (3), 467–476 (2025).
32. Mocanu, A. G. et al. Formulation and characterization of Ciprofloxacin loaded PLGA microspheres for applications in orthopedic infections. *Curr. Health Sci. J.* **43** (4), 306–310 (2017).
33. Rotman, S. G. et al. Development of bone seeker-functionalised microspheres as a targeted local antibiotic delivery system for bone infections. *J. Orthop. Translat.* **21**, 136–145 (2020).
34. Yuan, Z. et al. Injectable PLGA microspheres with tunable magnesium ion release for promoting bone regeneration. *Acta Biomater.* **85**, 294–309 (2019).
35. Qiao, Z. et al. Preparation, in vitro release and antibacterial activity evaluation of rifampicin and moxifloxacin-loaded poly(D,L-lactide-co-glycolide) microspheres. *Artif. Cells Nanomed. Biotechnol.* **47** (1), 790–798 (2019).
36. Cevher, E. et al. Characterization of biodegradable Chitosan microspheres containing Vancomycin and treatment of experimental osteomyelitis caused by methicillin-resistant Staphylococcus aureus with prepared microspheres. *Int. J. Pharm.* **317** (2), 127–135 (2006).
37. Norden, C. W., Myerowitz, R. L. & Keleti, E. Experimental osteomyelitis due to Staphylococcus aureus or Pseudomonas aeruginosa: a radiographic-pathological correlative analysis. *Br. J. Exp. Pathol.* **61** (4), 451–460 (1980).
38. Metsemakers, W. J. et al. Evidence-Based recommendations for local antimicrobial strategies and dead space management in Fracture-Related infection. *J. Orthop. Trauma.* **34** (1), 18–29 (2020).
39. Ghosh, S. et al. A potent antibiotic-loaded bone-cement implant against Staphylococcal bone infections. *Nat. Biomedical Eng.* **6** (10), 1180–1195 (2022).
40. Kuang, Z. et al. Osteogenic and antibacterial dual functions of a novel Levofloxacin loaded mesoporous silica microspheres/nano-hydroxyapatite/polyurethane composite scaffold. *Genes Dis.* **8** (2), 193–202 (2021).
41. Mir, M., Ahmed, N. & Rehman, A. U. Recent applications of PLGA based nanostructures in drug delivery. *Colloids Surf. B Biointerfaces*. **159**, 217–231 (2017).
42. Tseng, T. H. et al. A simple method to improve the antibiotic elution profiles from polymethylmethacrylate bone cement spacers by using rapid absorbable sutures. *BMC Musculoskelet. Disord.* **23** (1), 916 (2022).
43. Masters, E. A. et al. Evolving concepts in bone infection: redefining biofilm, acute vs. chronic osteomyelitis, the immune proteome and local antibiotic therapy. *Bone Res.* **7**, 20 (2019).
44. Kazimierczak, P. et al. Novel chitosan/agarose/hydroxyapatite nanocomposite scaffold for bone tissue engineering applications: comprehensive evaluation of biocompatibility and osteoinductivity with the use of osteoblasts and mesenchymal stem cells. *Int. J. Nanomed.* **14**, 6615–6630 (2019).
45. Yang, J. et al. Current opinions on the mechanism, classification, imaging diagnosis and treatment of post-traumatic osteomyelitis. *Chin. J. Traumatol.* **24** (6), 320–327 (2021).
46. Depypere, M. et al. Pathogenesis and management of fracture-related infection. *Clin. Microbiol. Infect.* **26** (5), 572–578 (2020).
47. Magnan, B. et al. Acrylic bone cement: current concept review. *Musculoskelet. Surg.* **97** (2), 93–100 (2013).
48. Mills, D. K. et al. Studies on the cytocompatibility, mechanical and antimicrobial properties of 3D printed poly(methyl methacrylate) beads. *Bioact Mater.* **3** (2), 157–166 (2018).
49. Wassif, R. K. et al. Recent advances in the local antibiotics delivery systems for management of osteomyelitis. *Drug Deliv.* **28** (1), 2392–2414 (2021).
50. Krizsán, G. et al. Investigation of the effect of rifampicin resistance and risk factors on recovery rates after DAIR procedure in patients with prosthetic joint infection. *J. Orthop. Surg. Res.* **18** (1), 611 (2023).

Author contributions

Author LG.S (First Author) and ZW.Q(Corresponding authors): Conceptualization, Methodology, Software, Investigation, Formal Analysis, Writing - Original Draft.Author WP.Z and HF.J: Methodology, Software, Investigation, Writing - Review & Editing.Author HQ.M and X.M: Investigation, Formal Analysis, Writing - Review & Editing.Author PJ.Z、ZP.Y and HH.S: Investigation, Resources, Writing - Review & Editing.All authors reviewed the manuscript.

Funding

The study was supported by Ningxia Natural Science Foundation (2023AAC02064) and National Natural Science Foundation of China (82460431).

Declarations

Competing intrests

The authors declare no competing interests

Ethics approval and consent to participate

All experimental procedures were performed in accordance with the guidelines of the Institutional Animal Care and Use Committee of Ningxia Medical University and ethical approval was obtained for the animal experiments conducted in the study(Certificate number:2020-0001), following the guidelines of the US National Institutes of Health and the Animal Research Reporting In Vivo Experiments (ARRIVE).

Additional information

Supplementary Information The online version contains supplementary material available at https://doi.org/10.1038/s41598-025-14824-0.

Correspondence and requests for materials should be addressed to Z.Q.